International Journal of Modern Manufacturing Technologies
ISSN 2067–3604, Vol. XVI, No. 1 / 2024
https://doi.org/ 10.54684/ijmmt.2024.16.1.39

EVALUATION OF SURFACE DETERIORATION RESULTING FROM THERMAL FATIGUE IN THE OPERATIONAL STATE OF AN H13 PRESSURE DIE CASTING DIE

Girisha Vijayapura Achappa, Hosahally Murthy Balaji Darshan, Bharatish Achutarao, Kirthan Lakshmi Narayana Murthy Jayalakshmi, Keshav Manjunath

Department of Mechanical Engineering, RV College of Engineering, Autonomous Institution affiliated to VTU, Belagavi, Bengaluru 560059, India

Corresponding author: Bharatish Achutarao, bharatisha@rvce.edu.in

Abstract: The failure rate of pressure die casting dies is increasing due to cracks on the die surfaces, leading to thermal fatigue and fracture. This paper aims to investigate the thermal fatigue failure of H13 die-casting die in running conditions by measuring the surface crack dimensions at core and cavity zones of the die during regular intervals of the die-casting process. The effect of length and width of the cracks on the die surface concerning coolant channel positions was analyzed. Transient thermal analysis was performed to investigate the temperature distribution, principal stress and total deformation of the die concerning to the coolant channel position using ANSYS. The maximum deformation of core insert was 0.0094 mm. Zone C of the core insert, which was 223.52 mm from the coolant channel location and corresponding to 139,237 cycles, had the longest crack, measuring 18.98 mm. Owing to greater temperature gradients, Zone Z of the cavity insert, which is situated 76.25 mm from the coolant channel, had the largest crack width, measuring 0.29 mm. The durability of the die casting die obtained from the numerical model (2.8×10^5 cycles) was in agreement with experimental studies (2.89×10^5 cycles).

Key words: pressure die casting; surface cracks, thermal fatigue, coolant channel position

1. INTRODUCTION

Thermal fatigue cracks commonly occur on the die surfaces which are exposed to cycles of high-temperature gradients and significantly reduce the ability of the dies to withstand high thermal loads. The development of local plastic strain on the die's surface during each casting cycle is what causes the thermal cracks, and this is a sign of a low-cycle fatigue process. During the procedure, they begin as tiny heat-checking cracks and grow larger [1]. During the cold phase of the die-casting cycle, high tensile stresses are applied to the die surface, which results in local plastic deformation, crack nucleation, and propagation throughout the course of the following cycles [2]. In the high-pressure die-casting process, the primary source of thermal loading, that significantly influences the occurrence of cracks is cyclic temperature fluctuations [3]. These cracks are closer to the die gate where temperature gradients are larger because of the higher melt temperature. Cracks also appear early in the areas of high-stress concentration and tend to develop deeper and longer over future cycles [4]. Encouraging an effective cooling channel at the base and enhancing the thermal stability of mechanical characteristics at operating temperatures can both helps to prolong the life of high-pressure die-casting dies [5]. Die life is generally measured in terms of "shots" or the number of cycles per die, with a range of 20,000 to 200,000 shots considered to be standard. Understanding the cyclic nature of the die-casting dies' surface becomes essential since the beginning section of the casting cycle contains the most severe thermal cyclic circumstances [6]. It is crucial to create a precise numerical model to predict die failure while taking into account the different failure modes. Therefore, measuring the dimensions of cracks on castings and estimating the level of crack formation and die thermal fatigue life would be more feasible.

According to Klobcar et al. [7], the length of the cracks was nearly equivalent to the depth of the decarburized layer formed on H13 die steel. Long A et al [8] reported that when the die cycle was frequently interrupted by cooling the H13 tool steel die to room temperature, wider and deeper cracks were developed on the die surface. The surface temperature of the shot plate was varied between 240°C and 500°C. Pawlowski et al [9] found that

the failure of aluminium alloy die casting occurred after very few shots instead of a guaranteed number of thousand shots leading to premature failure. This was mainly attributed to the formation of cracks in die casting due to low fracture toughness and improper heat treatment. Riccardo G et al [10] found that low-cycle fatigue testing of H13 steel specimens carried out at high temperature range of 500ºC – 550ºC resulted in multiple crack nucleation. Srivastava A et al [11] reported that an increase in temperature and thermal gradient caused a decrease in the number of die-casting cycles. Hassan et al. [12] utilized the strain at the specimen edge or the weakest point to correlate the number of die-casting cycles to crack initiation. They found that the progressive softening of tool steels during thermal cycling and subsequent stress concentration was the reasons for crack formation on the surface of the dies [13]. According to Singh et al. [14], the development of an air gap at the casting-die's interface lowers the heat transfer rate and increases the solidification time which in turn results in initiation of cracks. Yavuz et al. [15] investigated the effect of several coolant channel outlets in the dies for enhanced flow rate resulting in optimal cooling performance of the high-pressure die casting dies. The flow rate of the cooling air was significantly influenced by the inlet count (2), the pressure of the cooling channel (600 kPa) and the ratio between the inlet and outlet areas (0.5).

Studies have shown that the length of cracks is nearly equivalent to the depth of the decarburized layer formed on H13 die steel, while the frequency of die cycle interruption and air gaps between molten casting-die interfaces can also affect crack initiation. In high-pressure die casting, a number of coolant channel outlets in the dies can improve cooling efficiency and flow rate. It is essential to comprehend the cyclic nature of the die-casting dies' surface because the die casting cycle presents the most extreme thermal cyclic conditions. Factors affecting crack formation include high tensile stresses during the cold phase of the cycle, low fracture toughness and improper heat treatment of die casting, multiple crack nucleation at high temperatures, and an increase in cracks with higher thermal gradients. Enhancing cooling performance through an efficient cooling channel and improving the thermal stability of mechanical characteristics at operating temperatures can help prolong die life.

The purpose of this research was to investigate how die casting cycles affects crack size and shape during the casting process using an AISI A681 H13 steel die and AA383 alloy. Generating an accurate numerical model to forecast die failure and measuring crack dimensions on castings can help estimate the extent of crack formation and thermal fatigue life of dies. The researchers used an Auselese digital microscope to measure the dimensions of cracks on the die core and cavity surfaces. Performed a fatigue analysis of the die inserts by using the ANSYS V17.2 finite element package and used Paris Law to determine the experimental fatigue life, which they validated with a numerical model.

2. DESIGN AND MODELLING OF THE DIE

2.1. Number of cavities and tonnage requirement

Considering the component production required per month to be 50,000 pieces, loading of the die to be 6 days per week, number of the component produced per day is 2000, number of shifts per day to be 3, then, the number of shots per shift is evaluated as (8×60)/cycle time=720 shots per shift and the cycle time is 40 s per component. Hence, the number of components per shot = 2,000/(3×720) = 0.925 ~ 1. Thus, a single cavity die was adopted.

The projected area of the component is 86,520 mm^2, then, the projected area including the overflows and feeding system is 86,520×1.2=103.824 mm^2. Considering the specific injection pressure to be 60 MPa, the tonnage requirement is 86,520×4.8 (80% of injection pressure is considered) = 415,296 kg = 415.296 t. The security coefficient was set as 1.2, then, the locking tonnage required was 415.296×1.2 = 498.4 t ≈ 500 t. Thus, the 850 t HPDC (high pressure die casting) machine was used. The designed models of the core and cavity are shown in Figs. 1(a) and (b), respectively. The aluminium die casted component for street lighting application is as shown in Fig 1 (c).

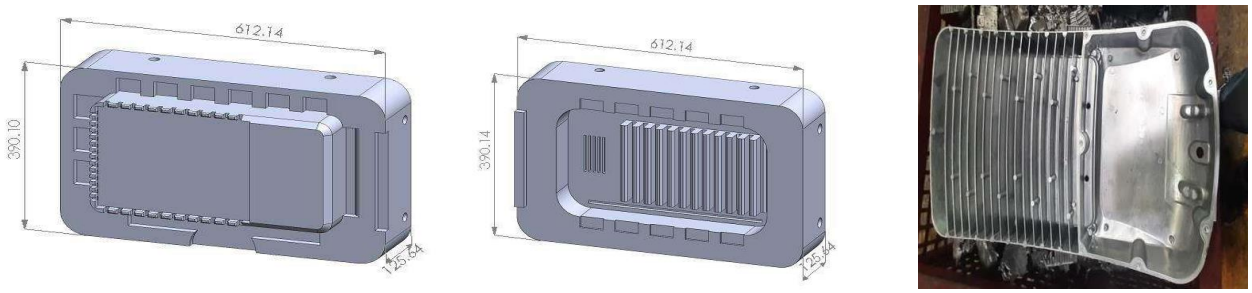

a. Core insert b. Cavity insert (c) Aluminium die-casted component

Fig. 1. Die inserts and casting component

2.2. Material properties

The exceptional hardness, abrasion resistance, and resistance to heat-checking cracks of AISI A681 H13 steel make it a popular choice for die-casting dies. The chemical composition of the AISI A681 H13 die steel is shown in Table 1. The mechanical properties of H13 die steel at room temperature are shown in Table 2. The standard heat treatment procedure for the die was as follows: The die billet was preheated to 650 °C and then nitrided at 830 °C. The austenitizing process was then carried out at 960 °C. Air and pressurized gas were used to quench the dies. Since the thickness of the die was greater than 130 mm, it was quenched with forced air and pressurized gas at 29 °C and then quenched with oil at 470 °C. The die was cooled in still air from 55 °C to 60 °C to increase the toughness and thermal fatigue resistance. The tempering at 590°C was immediately performed followed by quenching. Then, it was gradually cooled to room temperature. The melt is then degassed followed by remelting of top surface of the die billet using the Vacuum-Arc-Remelting (VAR) method. A hardness of 43 HRC was found from Rockwell's hardness test. The impact toughness of H13 steel was measured using a Charpy impact test, and the absorbed impact energy was found to be 15.2 J.

Table 1. Nominal composition of H13 die steel (mass%), [5]

Cr	Mo	Si	V	C	Ni	Cu	Mn	P	S	Fe
4.75-5.50	1.10-1.75	0.80-1.20	0.80-1.20	0.32-0.45	0.3	0.25	0.20-0.50	0.03	0.03	Bal.

Table 2. Mechanical properties of H13 die steels, [5]

Properties	**Units**
Elasticity modulus	215 GPa
Yield strength	1,230 MPa
Tensile strength	1,430 MPa
Poisson's ratio	0.28
Thermal expansion	11.42×10^{-6} (ºC)
Thermal conductivity	27.61 $W\cdot m^{-1}\cdot K^{-1}$
Density	7,750 kg m^{-3}
Specific gravity	7.75

3. MEASUREMENT OF DIMENSIONS OF CRACK INDUCED DURING THE DIE-CASTING CYCLE

The die-casting process was carried out with a die stroke of 760 mm, a locking force of 8500KN and a shot force of 660KN. The pouring temperature of the aluminium molten metal was 700ºC during the operation. The coolant was continuously circulated through coolant channels at 28ºC for lubrication and heat rejected from the surface of the die. The die-loading parameters are shown in Table 3. The chemical composition of A383 is shown in Table 4, and the properties of AA383 alloy at room temperature are shown in Table 5.

Table 3. Die loading parameters

Parameter	Value
Weight of each shot casting	2.4 kg
Pouring temperature	700 ºC
Preheated die temperature	300 ºC
Injection pressure	60 MPa
Mean filing time of molten metal	45 m·s-1
Cycle time	40 s

Table 4. Nominal ccompositions of A383 alloy (mass %) [6]

Al	Cu	Mg	Fe	Sn	Ni	Zn	Mn	Si
77.3-86.5	2-3	0.1	1.3	0.15	0.3	3.0	0.5	9.5-11.5

Table 5. Mechanical and thermal properties of A383 alloy [6]

Material	A383
Density of the melt	2,780 kg·m-3
Yield strength	150 MPa
Impact energy	4 J
Dynamic viscosity (μ)	1.2 mPa·s
Specific heat (Cp)	1,180 J·kg-1·°C-1
Thermal conductivity (K)	204 W·m-1·°C-1

The local sections of core and cavity die inserts with respect to their coolant channel positions are shown in Figs. 2 and 3, respectively. The surface of the die with respect to the coolant channel position was divided into four zones namely A, B, C, and D in the core insert and X, Y, and Z zones in the cavity insert. This can be visualized in the side views in Figs. 2 and 3.

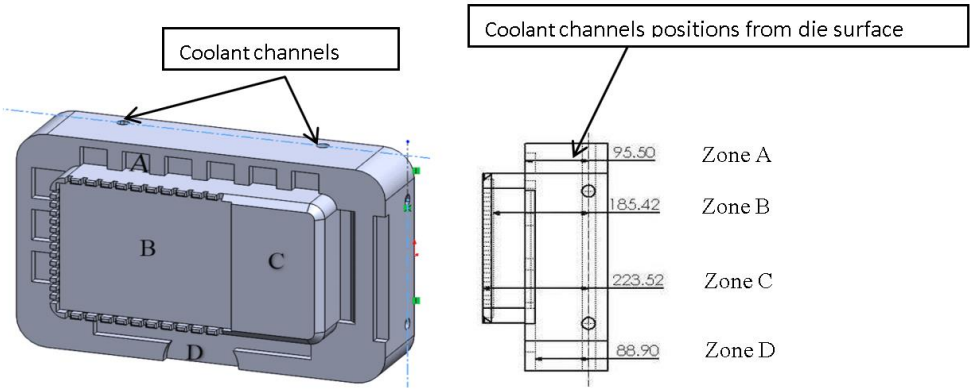

Fig. 2. Zones (A, B, C and D) with respect to coolant channel position on core insert

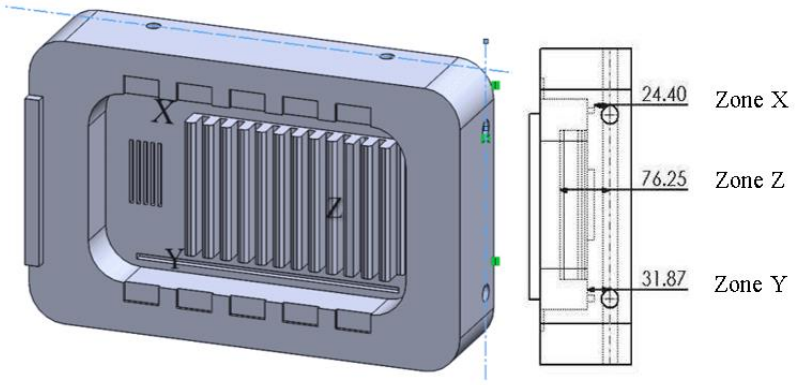

Fig. 3. Zones (X, Y and Z) with respect to coolant channel position on cavity insert

The microstructure of the die surface was obtained using an Auselese microscope and the crack dimensions were measured using the Hi-view software as shown in Figs. 4(a) and (b). These measurements were performed at the end of four intervals of die-casting cycles, i.e., 28,101; 69,437; 103,329 and 139,237.

3.1. Fatigue analysis of die-casting dies

The core and cavity die models were analyzed for fatigue failure using ANSYS 17.2 package. The die models were meshed using tetrahedron elements. The mesh size of 5 mm was adopted for the analysis of both core and cavity. The finite element model of core insert [Fig. 5(a)] comprises 70,351 nodes and 42,421 elements and that of cavity insert [Fig. 5(b)] comprises 78,141 nodes and 45,320 mesh elements.

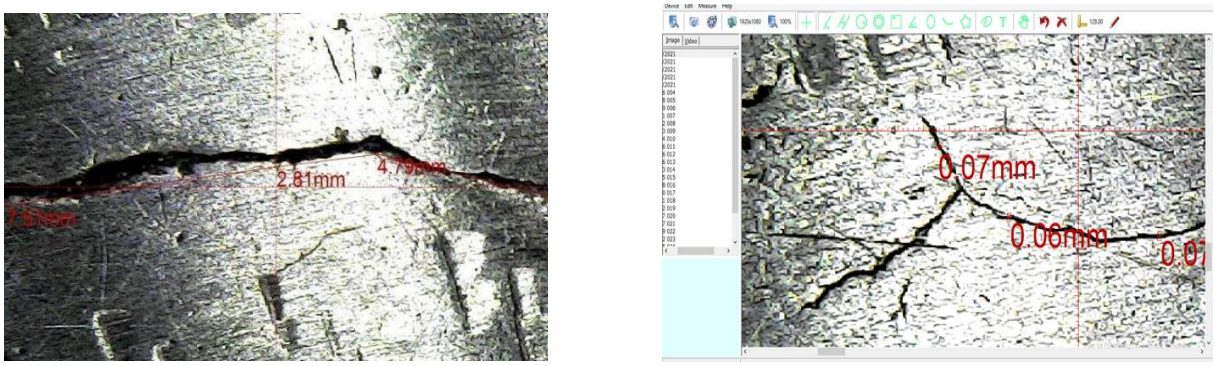

Fig. 4. Crack dimensions obtained on core (a) and cavity (b)

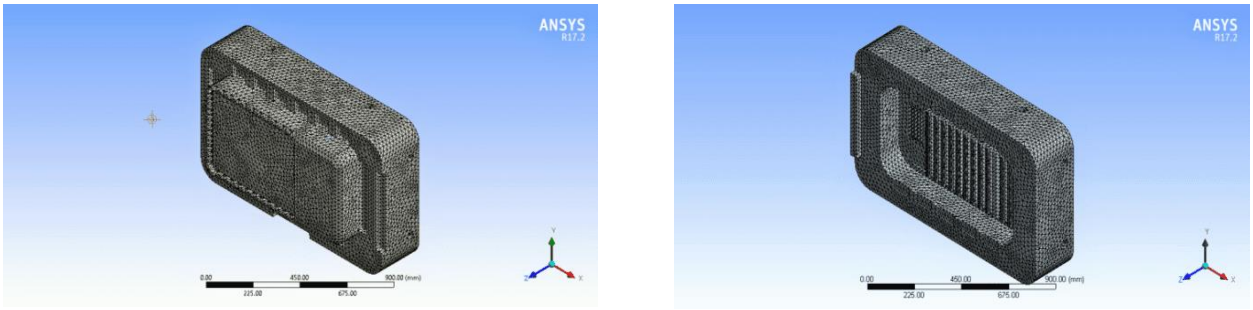

Fig. 5. Meshed models of core insert (a) and cavity insert (b)

The transient thermal analysis was performed to obtain the temperature distribution and thermal stresses produced due to thermal load caused by the injection of hot aluminium melt. The convection coefficient was computed using the basic principles of heat transfer as follows:
Reynolds number (Re) is computed by Eq. (1), [16]:

$$Re = \frac{\rho v L}{\mu} \tag{1}$$

where v is the flow velocity of the A383 melt, which is 45 $m \cdot s^{-1}$, and L is the characteristic length of the die surface, which is 0.395 m. The dynamic viscosity (μ) and density (ρ) of A383 aluminium melt are given in Table 5.
Prandtl number (Pr) is computed using Eq. (2)

$$\mathrm{Pr} = \frac{\mu C_p}{K} \tag{2}$$

where, Cp is the specific heat and K is the thermal conductivity of the aluminium melt (Table 5).
Nusselt number (Nu) under forced convection is computed using Eq. (3):

$$Nu = \frac{hL}{K} = 0.565\,(RePr)^{0.5} \tag{3}$$

where h is the convection coefficient, which is computed as 24.6×104 $W \cdot m^{-2} \cdot {}^{o}C^{-1}$.
The thermal boundary conditions such as surface temperature of 700 oC and the computed convection coefficient of 24.6×104 $W \cdot m^{-2} \cdot {}^{o}C^{-1}$ were adopted. The coolant temperature was maintained at 28°C. The fatigue analysis was carried out by adopting the boundary conditions such as injection pressure of 60MPa, a density of aluminium melt 2.375 $kg \cdot m^{-3}$, and a magnitude of aluminium melt flow velocity of 45 $m \cdot s^{-2}$ acting on the die surface. The rear end of the die inserts was fully constrained to obtain the maximum principal stresses at core and cavity zones.

4. RESULTS AND DISCUSSION

4.1. Responses of transient thermal and structural analysis

The temperature distribution along core and cavity inserts are as shown in Fig. 6(a)-(b). The temperature distributes in the range of 200 ^{0}C to 680 ^{0}C for both core and cavity inserts. The contour plots of total deformation

of cavity and core are shown in Fig. 7(a)-(b). The maximum deformation of core insert (0.0094 mm) is found to be higher than that of cavity insert (3.63×10-6 mm). The contour plots depicting the principal stresses at the identified zones on the core and cavity inserts are shown in Fig. 8(a) – (b). The scatter plots were obtained to analyze the effect of coolant channel position on the principal stresses, as shown in Fig. 9(a) – 9(b). Zone C of the core, which was 223 mm away from the coolant channel position, experienced the maximum principal stress of 796.08 MPa. Also, Zone Z of cavity which was 76.25 mm away from the coolant channel location, witnessed the maximum principal stress of 493.15 MPa. Therefore, higher stresses were induced at a position far away from coolant position. This variation was mainly attributed to the temperature difference between the internal and external surfaces of the dies. Also, the principal stresses were smaller than yield strength of H13 steel die.

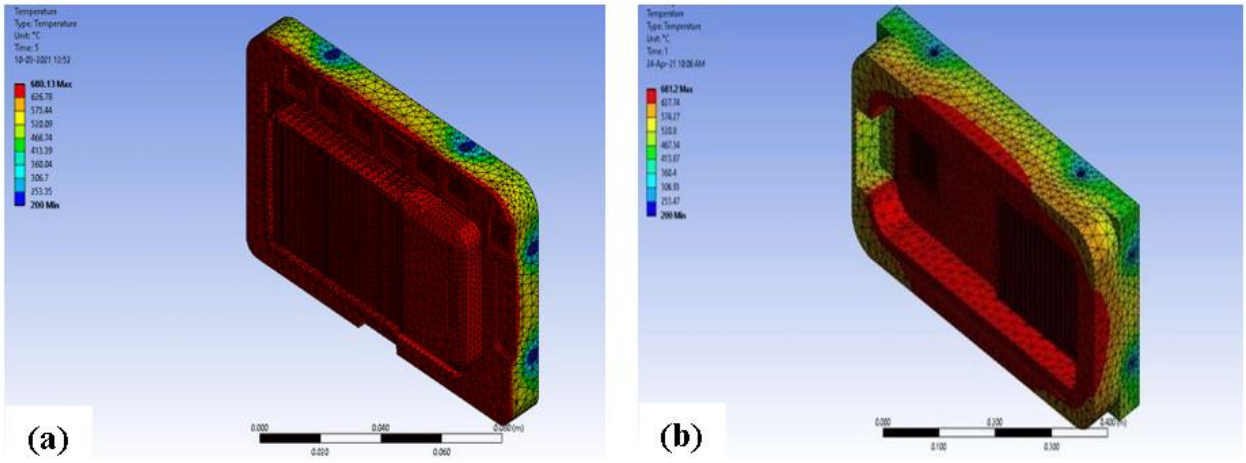

Fig. 6. Temperature distribution in core insert (a) and cavity insert (b)

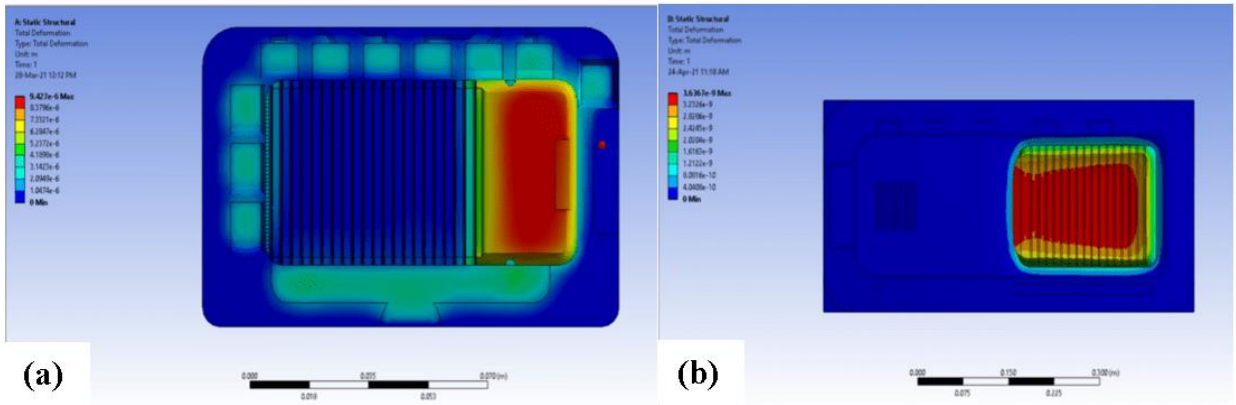

Fig. 7. Contours of total deformation of core (a) and cavity (b)

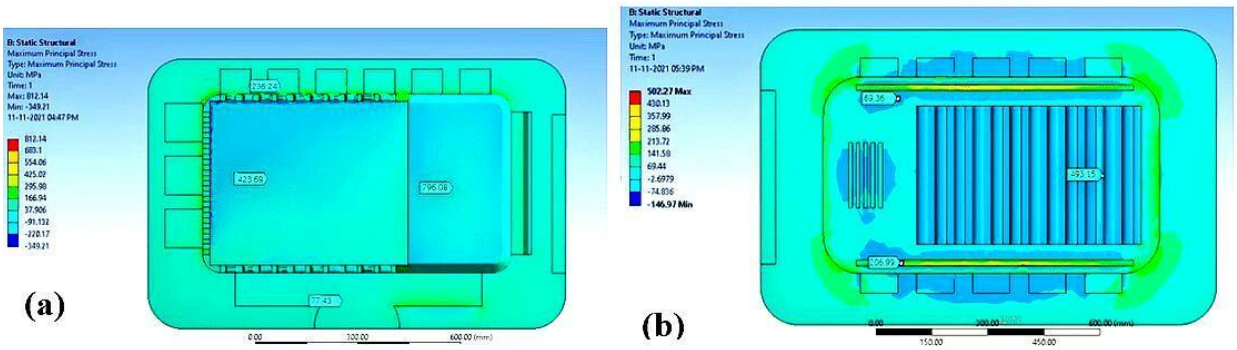

Fig. 8. Contour plot of maximum principal stress on core insert (a) and cavity insert (b)

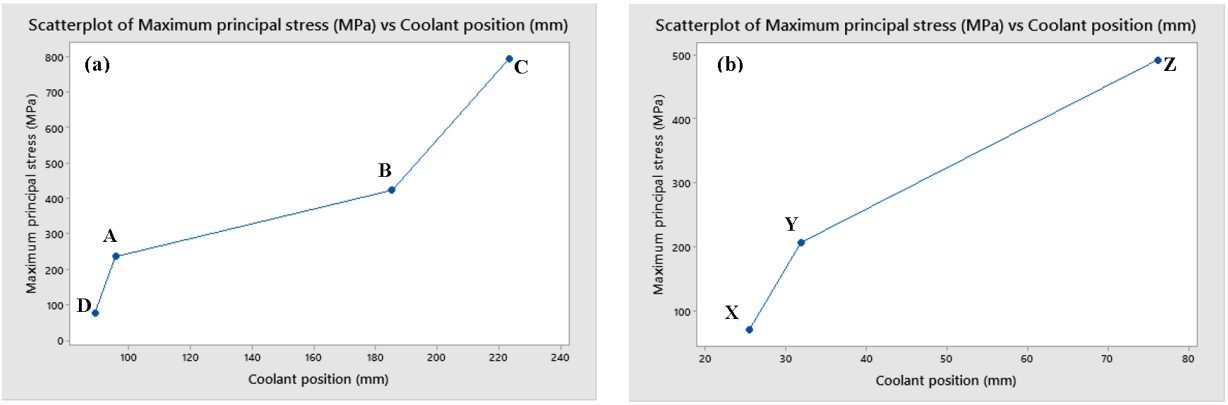

Fig. 9. Scatter plot of principal stresses at coolant channel positions on core (a) and cavity (b)

4.2. Crack lengths along coolant channel positions

The crack length obtained on the identified zones of die surface at intervals of die casting cycles during its operation is shown in Table 6.

Table 6. Crack length in different zones

Number of cycles		28.101	69.437	103.329	139.237
Zones	Coolant position (mm)	Crack length (mm)	Crack length (mm)	Crack length (mm)	Crack length (mm)
Crack length in zones of core insert					
A	95.5	0	0	2.19	6.4
B	185.42	5.04	6.72	10.56	14.33
C	223.52	8.14	12.14	16.84	18.98
D	88.9	2.22	4.32	6.6	9.83
Crack length in zones of cavity insert					
X	25.4	0	2.35	4.57	4.83
Y	31.87	0	5.3	7.61	10.7
Z	76.25	2.33	6.73	9.33	11.65

Figures 10 (a) and (b) show the predict crack length at different coolant channel locations at four intervals of die casting cycles on core and cavity inserts, respectively. Even after the completion of 69,437 cycles, Zone A didn't experience any cracks. But, when 1,03,329 cycles were completed, Zone A started to exhibit cracks which were of 2.19 mm long. Finally, after the completion of 139,237 cycles, Zone C showed the longest crack length of 18.98 mm and Zone A showed a shorter crack length of 6.4 mm. The microscopic image of the longest crack is shown in Fig. 13(a). The crack dimensions were measured using Hi-View software as shown in Fig. 13(b). Zone D and Zone B exhibited 9.83 mm and 14.33 mm crack length, respectively. Thus, the position of the coolant channel near Zone A could be beneficial due to chances of reduced failure. On the other hand, coolant channel position at the proximity of Zone C could be detrimental to the performance of dies at high pressure.

When 28,101 cycles were completed, no cracks were found in both the X and Y zones in the cavity. The only crack reported was in Zone Z with a length of 2.33 mm. After the completion of 69,437 cycles, X zone exhibited a shorter crack length of 2.35 mm and Z zone had longer crack length of 9.33 mm. When 103,329 cycles were completed, the X zone exhibited cracks of 4.57 mm long. The longest crack length of 11.65 mm was observed at zone Z of cavity insert after the completion of 139,237 cycles.

Table 7 shows the crack widths measured it different zones of the dies at different intervals of die casting cycles. Figure 12 illustrates the variation of crack width *vs.* the distance the coolant channel positions away from the surface of the core and cavity insert. Except zone A, the width of the cracks in the core inserts increased consistently with the increase of the distance away from the coolant channel positions during the 28,101 and 69,437 cycles without any significant variations. But, during the 103,329 and 139,237 cycles, all the zones exhibited a strong peak in the width of the cracks. During the end of the 139,237 cycle, Zone C witnessed the widest crack of 0.23 mm. In the cavity, during the 28,101 cycles, there were no cracks reported in both X and Y zones. Cracks of approximately 0.11 mm were identified in Zone Z. A sudden rise in crack width was noted from 69,437 cycles at all the three zones. Figure 13(a) shows the microscopic image of the widest crack. Figure 13(b) shows the widest crack of 0.29 mm at the end of 139,237 cycles in Zone Z which was 76.25 mm away from the

coolant position. The crack initiation was accelerated by gradual softening of die surface material during its operation, which was mainly due to the tempering of high-temperature aluminum alloy [4].

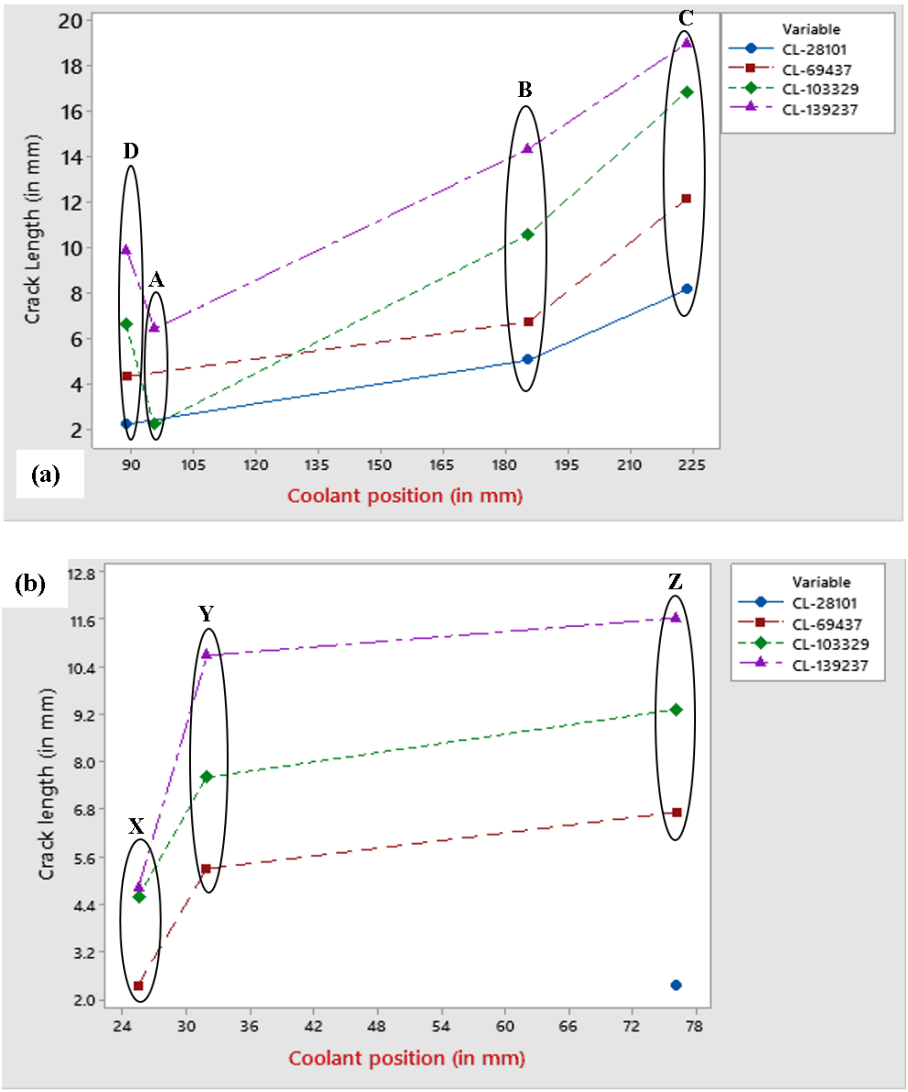

Fig. 10. Crack length in zones of (a) core and (b) cavity at intervals of die cycle

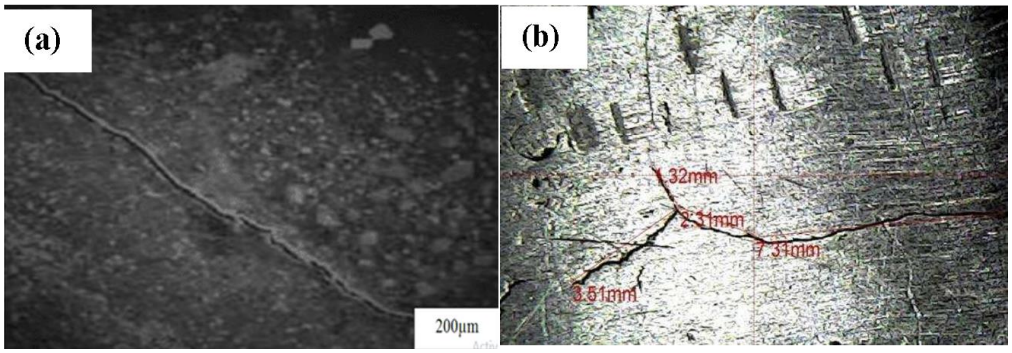

Fig. 11. Microscopic image of the longest crack (a), and (b)cracks measurement in Hi-View software

Table 7. Crack width in different zones of core and cavity

Number of cycles		28,101	69,437	103,329	139,237
Zones	Coolant position	Crack width (mm)	Crack width (mm)	Crack width (mm)	Crack width (mm)
Crack dimensions of core insert					

A	95.5	0	0	0.16	0.17
B	185.42	0.13	0.15	0.19	0.22
C	223.52	0.18	0.18	0.19	0.23
D	88.9	0.05	0.07	0.14	0.18
Crack dimensions of cavity insert					
X	25.4	0	0.16	0.16	0.23
Y	31.87	0	0.18	0.22	0.26
Z	76.25	0.11	0.24	0.25	0.29

5. FATIGUE LIFE PREDICTION OF DIE CASTING DIES

5.1. Fatigue analysis-numerical approach

Fatigue damage was computed by dividing the designed life by the available life. To connect the fatigue life to the stress state, S-N curve in a stress-fatigue life study was adopted. Thus, after accounting for fatigue loading type, mean stress effects, and multi-axial effects in the fatigue study [5], the "equivalent alternating stress" was utilized to query the fatigue S-N curve. The equivalent alternating stress is considered as the final computed quantity before estimating the fatigue life of a component. The analysis type adopted was stress life approach which addressed high cycle fatigue (>100,000 cycles); the fatigue life of materials was computed by subjecting it to different stress amplitudes. Figures 14(a) and (b) depict the fatigue life of a core and cavity insert, respectively. Goodman's mean stress theory was adopted to predict the die life (Fig. 15). The fatigue analysis performed using ANSYS indicate that the maximum number of cycles before the die failure occurred is 2.8×10^5.

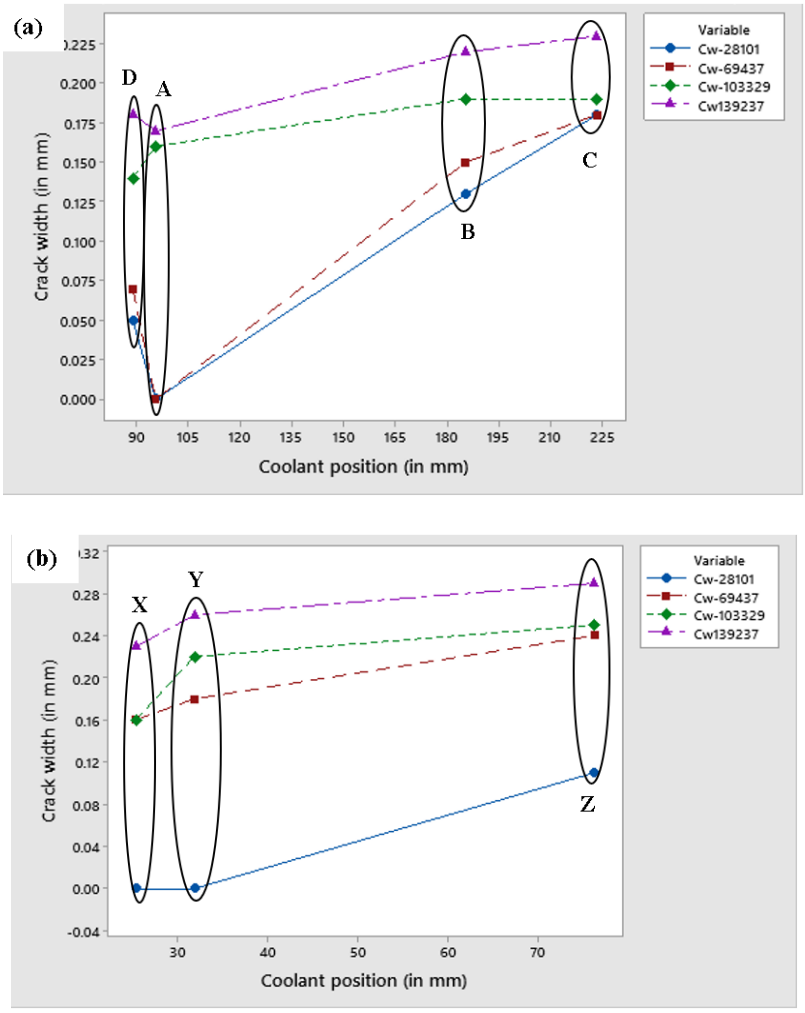

Fig. 12. Crack width on zones of core insert (a) and cavity insert (b)

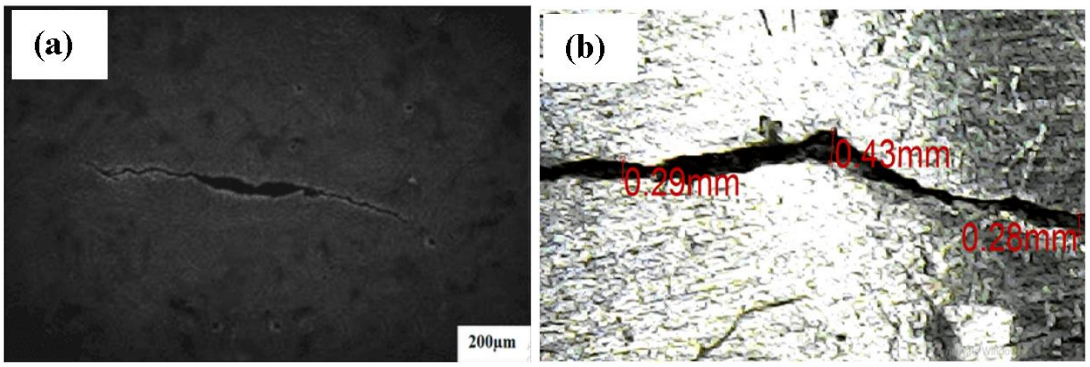

Fig. 13. Microscopic image of the widest crack (a) and crack measurement using Hi-view software (b)

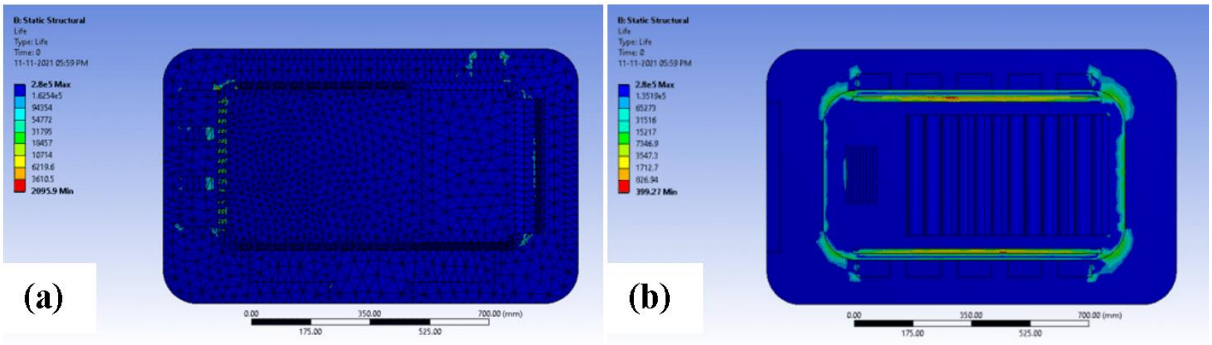

Fig. 14. Fatigue life of core (a) and cavity (b) insert

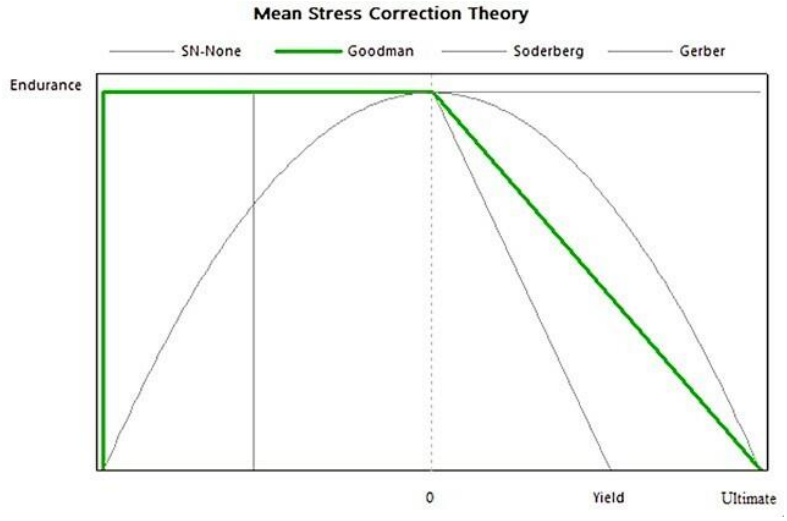

Fig. 15. Goodman mean stress curve

5.2. Validation of fatigue life of AISI A681 H13 die casting die

The number of failure cycles based on the size of the cracks formed on the surface of the die due to thermal fatigue was computed using Paris law. Based on the shape of the cracks formed on the surface of the die, the stress intensity factor is given by Eq. (4) [17, 18]:

$$Kf = \frac{2\times\Delta\sigma\times\sqrt{(\pi a_c)}}{\pi} \tag{4}$$

The stress intensity factor (Kf) for H13 die steel at 700 °C is as 83.6 MPa√m [17]. The tensile stress (Δσ) for H13 die steel at 700 °C is 396 MPa [18]. Therefore, the critical crack length (ac) was found to be 34.9 mm.
The number of failure cycles of the die was determined using Eq. (5):

$$Nf = \frac{a_o^{\left(1-\frac{n}{2}\right)}}{C\times\left[\frac{n}{2}-1\right]\times\left[\frac{2\times\Delta\sigma}{\sqrt{\pi}}\right]^n} \times \left\{1-\left(\frac{a_o}{a_c}\right)^{\left(\frac{n}{2}-1\right)}\right\} \tag{5}$$

The H13 die steel belongs to the ultrahigh strength steel group and C and n values for such steels can be found in [17, 20]. As previously stated, the size of pre-existing cracks (a_o) in heat-treated and surface-hardened H13 steel (extrusion dies) is typically in the range of 0.01-0.1 mm [17]. The initial crack length (a_o) was considered as 0.01 mm, the critical crack length (ac) was 34.9 mm, and the material constants C and n were 1.6×10^{-12} and 2.85, respectively [17]. These material constants were compared with other grades of steel as shown in Table 8. The number of cycles (N_f) before the die failure was found to be $289383.43 \approx 2.89\times10^5$. Thus, the computed fatigue life was in agreement with the numerical results.

Table 8. Material constants C and n for different grades of steel [17, 20]

Steel type	n	C	N_f	a_c [mm]
S420	3.03	8.31×10-13	275200	23.152
S235	2.50	3.34×10-11	442200	36.056
H13 (current research)	2.85	1.6×10-12	289384	34.9

6. CONCLUSION

This study focused on the effect of surface cracks on the thermal fatigue behavior of AISI A681 H13 steel die. The length and width of the cracks on the die surface with respect to coolant channel positions was analyzed. Transient thermal analysis was performed to investigate the temperature distribution, principal stresses, and total deformation of the die. The maximum deformation of core insert was 0.0094 mm. The maximum principal stress of 796.08 MPa was reported at Zone C of core insert and 493.15 MPa at Zone Z of cavity insert. The maximum crack length of 18.98 mm was observed at Zone C of core and 11.65 mm in Zone Z of cavity, both the zones being farthest from the coolant channel position. Similarly, the maximum crack width of 0.23 mm on the core and 0.29 mm on the cavity, both these zones being farthest from the coolant channel position. Thus, longer and wider cracks were found at zones far away from the coolant channel positions. The durability of the die casting H13 steel die obtained numerically (2.8×10^5 cycles) agreed well with experimental studies (2.89×10^5 cycles).

Conflicts of Interest: There is no conflict of interest.

REFERENCES

1. Persson A., (2003), *Tool failure in die casting*, Ph.D. Thesis, Department of Materials Science, Uppsala University, Sweden.
2. D. Klobčar L, Kosec B., Kosec J., (2012), *Thermo fatigue cracking of die casting dies*, Engineering Failure Analysis, 20:43-53, https://doi.org/10.1016/j.engfailanal.2011.10.005.
3. Kosec B., Kosec G., Sokovic M., (2007), *Temperature field and failure analysis of die-casting die*, Achievements of Materials Science and Engineering, 28(3), 182-187.
4. Muhic M., Tušek J., Kosel F., (2010), *Thermal fatigue cracking of die-casting dies*. Metalurgija, 49(1), https://hrcak.srce.hr/40242.
5. Girisha VA., JoshiM M., Kirthan LJ., (2019), *Thermal fatigue analysis of H13 steel die adopted in pressure-die-casting process*, Sādhanā, 148, https://doi.org/10.1007/s12046-019-1111-3.
6. Persson A., Hogmark S., Bergström J., (2004), *Temperature profiles and conditions for thermal fatigue cracking in brass die casting dies*, Journal of Materials Processing Technology, 152(2), 228-236, https://doi.org/10.1016/j.jmatprotec.2004.04.241.
7. Klobcar D., Tusek J., (2008), *Thermal stresses in aluminium alloy die casting dies*, Computational Materials Science, 43(4), 1147-1154, https://doi.org/10.1016/j.commatsci.2008.03.009.
8. Long A., Thornhill D., Armstrong C., (2012), *Predicting die life from die temperature for high pressure dies casting aluminium alloy*, Applied Thermal Engineering, 44, 100-107, https://doi.org/10.1016/j.applthermaleng.2012.03.045.
9. Pawłowski B., P Bala., Tokarski T., (2013), *Premature cracking of dies for aluminium alloy die-casting*, Archives of metallurgy and materials, 58:1275-1279, http://dx.doi.org/10.2478/amm-2013-0147

10. Riccardo G., Rivolta B., Gorla C., (2021), *Cyclic behaviour and fatigue resistance of AISI H11 and AISI H13 tool steels*. Engineering Failure Analysis, 121: 105096, https://doi.org/10.1016/j.engfailanal.2020.105096.
11. Srivastava A., Joshi V., Shivpuri R., (2004*), Computer modeling and prediction of thermal fatigue cracking in die-casting tooling*. Wear, 256(1-2), 38-43, https://doi.org/10.1016/S0043-1648(03)00281-3.
12. Abdulhadi HA., Aqida SN., Ishak M, (2016), *Thermal fatigue of die-casting dies*, An overview. MATEC Web of conference, 74(5), 00032, https://doi.org/10.1051/matecconf/20167400032
13. Persson A., Hogmark S., Bergström J., (2004), *Simulation and evaluation of thermal fatigue cracking of hot work tool steels*, International Journal of Fatigue, 26(10), 1095-1107, https://doi.org/10.1016/j.ijfatigue.2004.03.005.
14. Singh D., Navaneeth V., Lee J., (2011). *Developing a localized squeeze cooling technique for improved casting solidification*, International Journal of Metal casting, 5, 65–79. https://doi.org/10.1007/BF03355472.
15. Yavuz H., Ertugrul O., (2020), *Numerical analysis of the cooling system performance and effectiveness in aluminium low-pressure die casting*. International Journal of Metal casting, https://doi.org/10.1007/s40962-020-00446-x
16. W.M. Rohsenow., J.P. Hartnett., Y.I Cho., (1998), *Handbook of Heat transfer, 3rd edition*, McGraw Hill, ISBN 0-07-053555-8.
17. Sayyad Q., Tasneem P., Siddiqui R A., (2007), *Sensitivity analysis in life prediction of extrusion dies*, Journal of Achievements in Materials and Manufacturing Engineering, 25(1).
18. Arsic D., Lazić V., Nikolić R., (2018), *Mechanical properties of hot-work tool steel at elevated temperatures*, In: Proc. 23rd International Seminar of Ph.D. Students "SEMDOK 2018", Western Tatras-Zuberec, Slovakia.

Received: November 11th, 2023 / Accepted: June 15th, 2024 / Paper available online: June 20, 2024 © International Journal of Modern Manufacturing Technologies.